

Deep Learning Algorithms for Hedging with Frictions*

Xiaofei Shi[†]

Daran Xu[‡]

Zhanhao Zhang[§]

April 18, 2022

Abstract

This work studies the deep learning-based numerical algorithms for optimal hedging problems in markets with general convex transaction costs on the trading rates, focusing on their scalability of trading time horizon. We implement two popular deep learning algorithms, the FBSDE solver introduced in the spirit by Han, Jentzen, and E (2018) and the deep hedging algorithm pioneered by Buehler, Gonon, Teichmann, and Wood (2019), and compare their performances with the leading-order approximations. In summary, the FBSDE solver only performs well under short trading horizons, whereas the deep hedging algorithm has stable and reliable performance for short and moderately long trading horizons. For long trading horizons, we propose a “pasting” algorithm to aggregate the leading-order approximations and the deep learning-based algorithms together, hence fully utilizing both of their advantages.

1 Introduction

As observed in many empirical papers, markets are imperfect, meaning that arbitrary quantities cannot be traded immediately at the quoted market price because of taxes, regulations, and the limited liquidity of the assets. Typical examples include linear transaction taxes as well as fixed transaction costs. As reported and studied in [3, 4, 6, 42], empirical estimates of actual transaction costs typically correspond to a 3/2-th power of the order flow. Accordingly, the large trading volume quickly impacts the market liquidity, which, in turn, drastically changes the agents’ behaviors. Hence, optimally scheduling the order flow in anticipation of market liquidity shortage is crucial.

There is a large body of literature on optimal execution strategies as well as dynamic portfolio optimization models with market illiquidity and price impacts, see, e.g. [7, 20, 22, 38, 41, 43, 53], and with recent results in [9, 24, 31, 54]. By assuming the transaction costs correspond to the square of the size of the order flow, the optimal trading policy can be given in a closed-form, as shown in [24, 41]. However, no closed-form solution is available under general nonlinear transaction costs with general market dynamics. To obtain tractable results, researchers then focus on the *small* costs limit, as in [5, 10, 31, 40, 45, 53, 54]. These elegant asymptotic formulas were proved rigorously by [2, 35, 39, 53]. Two important follow-up questions therefore arise. The first one is about the quality of the leading order approximation, which needs to be well-studied and quantified, especially in empirical examples. The second is about the smallness assumption, whether that is an absolute or a relative quantity.

*The authors thank Jiequn Han, Ruimeng Hu, Johannes Muhle-Karbe, Junru Shao, and Xunyu Zhou for fruitful discussions. Part of the work is supported by the MA Mentored Research Program in Statistics at Columbia University.

[†]Columbia University, Department of Statistics, email xs2427@columbia.edu.

[‡]Columbia University, Department of Statistics, email dx2207@columbia.edu.

[§]Columbia University, Department of Statistics, email zz2760@columbia.edu.

From the numerical side, recent advances in highly accurate machine learning models have introduced powerful new tools for studying high-dimensional optimization problems, such as hedging with frictions. The FBSDE solver, developed by Han, Jentzen, and E in [32], can solve a dynamic portfolio optimization problem by finding the solution to a BSDE system. For the first time, this algorithm overcame the curse of dimensionality in numerical solutions to high-dimensional SDE and associated PDE, as pointed out by [11, 28]. The convergence analysis is established by [33] under the same short-term existence assumptions in [21]. At a higher level, the FBSDE solvers find the solution of the FBSDEs through a *supervised learning* framework, since the accuracy of the terminal value of the backward components is served as the goal functional of the algorithm. However, this algorithm does not scale well with the trading time horizon and the time discretization. For calibrated trading parameters as in [26], the time horizon for the algorithm to work is required to be unreasonably small. In the meantime, with the development of modern model-free techniques, *reinforcement learning* algorithms are also widely used in single-agent optimization problems. Indeed, as shown in the groundbreaking papers [12, 14, 15, 16, 34, 36, 37, 44, 47, 49, 50], we treat the utility functions as targets and directly parametrize and learn the optimal trading policy. Moreover, reinforcement learning frameworks are introduced and analyzed rigorously in [56, 57]. Therefore, just like in [44], a natural question is how these methods compare in practice, and our goal is to understand and compare the two types of methods, especially the advantages and drawbacks of supervised learning and reinforcement learning algorithms.

This paper studies the optimal hedging problem in frictional markets in a general setting. First, we explore different machine learning architectures, including the FBSDE solver and the deep hedging algorithms. We implement both methods, document the tuning procedures, and discuss their advantages and disadvantages. Then we compare our numerical results with the asymptotic formulas in a Bachelier model for the price dynamics. These comparison results help explain the asymptotic formula and provide us with ideas on the usage of each method in practice. Finally, we propose a “pasting” algorithm to fully utilize the convenience of the leading-order formula and the accuracy of the learning-based algorithms. In addition, this is preliminary documentation for the numerical methods that could be generalized to solve Radner and Nash equilibrium models, where several agents interact strategically, alongside with [16, 26].

The rest of the paper is organized as follows. First, in Section 2, we introduce the market model with frictions, the preference for individual agents, and the admissible strategies. Then, the FBSDE solver and deep hedging algorithms are introduced in Section 3, with details on the implementations and comparisons. Finally, we compare the performance of different learning-based algorithms and the leading-order approximation formula in two Bachelier models in Section 4. In summary, the leading-order approximations work well under long trading horizons, while it deviates from the ground truth by a significant amount only shortly before maturity. On the other hand, the FBSDE solver only performs well under short trading horizons, while it fails to work in long trading horizons. In contrast, the deep hedging algorithm has stable and reliable performance for short and moderately long trading horizons, which shows great potential in the deep reinforcement learning algorithms. Based on these observations, we propose our “pasting” algorithm. For better readability, the derivation of leading-order approximations and all proofs are collected in Appendix A.

Notation. We fix a filtered probability space $(\Omega, \mathcal{F}, (\mathcal{F}_t)_{t \in [0, T]}, \mathbb{P})$ with finite time horizon $T > 0$, where the filtration is generated by a 1-dimensional standard Brownian motion $W = (W_t)_{t \in [0, T]}$. For $p > 1$, we write \mathbb{H}^p for the \mathbb{R} -valued, progressively measurable processes $X = (X_t)_{t \in [0, T]}$ with $\|X\|_{\mathbb{H}^p} := \left(\mathbb{E} \left[\left(\int_0^T |X_t|^2 dt \right)^p \right] \right)^{1/p} < \infty$.

2 Model Setup

Here, we assume the randomness in the market is generated by the 1-dimensional Brownian motion $(W_t)_{t \in [0, T]}$. Suppose we receive a cumulative random endowment as

$$d\zeta_t = \xi_t dW_t, \quad \text{for a general process } \xi \in \mathbb{H}^2.$$

There are two assets in the market for us to hedge the risk, the first one is safe, with price normalized to one, and the second is risky, with general dynamic

$$dS_t = \mu_t dt + \sigma_t dW_t, \tag{2.1}$$

where the expected return process satisfies the no-arbitrage condition $\mu = \sigma\kappa$ for a market price of risk $\kappa \in \mathbb{H}^2$. One readily verifies that the Bachelier models and Geometric Brownian motions satisfy this requirement.

Transaction costs. A popular class of models originating from the optimal execution literature focuses on absolutely continuous trading strategies, cf. [3, 4],

$$\varphi_t = \varphi_{0-} + \int_0^t \dot{\varphi}_u du, \quad t \geq 0,$$

and penalizes the trading rate $\dot{\varphi}_t = d\varphi_t/dt$ with an *instantaneous transaction cost* $\lambda_t G(\dot{\varphi}_t)$. With proper definition of matrix-valued operation, this formulation of transaction costs can be generalized to multiple risky assets with cross-asset costs.

G is used to model the “shape” of transaction costs. Portfolio choice problems for the most tractable quadratic specification $G(x) = x^2/2$ are analyzed in models by [5, 13, 25, 30, 45, 51]. In the small transaction costs limit as in [10, 18, 31], single-agent models are solved explicitly for the more general power costs $G(x) = |x|^q/q$, $q \in (1, 2]$ proposed by [3]. Below, we introduce the general smooth convex cost functions G as studied in [26, 29], which includes the special examples mentioned above:

Assumption 2.1. (i) The transaction cost $G : \mathbb{R} \rightarrow \mathbb{R}_+$ is convex, symmetric, and strictly increasing on $[0, \infty)$, differentiable on $(0, \infty)$, and satisfies $G(0) = 0$;

(ii) The derivative G' is also strictly increasing and differentiable on $(0, \infty)$ with $G'(0) = 0$;

(iii) There exist constants $C > 0$, $K \geq 2$ and $x_0 > 0$ such that

$$|(G')^{-1}(x)| \leq C(1 + |x|^{K-1}) \text{ for all } x \in \mathbb{R}, \quad G''(x) \leq C \text{ for all } |x| > x_0.$$

The power costs and their linear combinations are included, and the proportional costs can also be studied as the singular limit of power costs with the power approaching 1.

The process λ models the level of the transaction costs parameter. Like in the partial-equilibrium model of [45], we allow the transaction cost to fluctuate randomly over time:

$$\lambda_t = \lambda \Lambda_t, \quad t \in [0, T]. \tag{2.2}$$

Here, the constant $\lambda > 0$ modulates the magnitude of the cost (this scaling parameter will be sent to zero in the small-cost asymptotics, where explicit formula is available as in [31, 17]. We restate this results in Appendix A.2). The *strictly positive* stochastic processes $(\Lambda_t)_{t \in [0, T]}$ describes the fluctuations of liquidity over time, and allows to model “liquidity risk” as in [1], for example.

Preferences and Admissible Strategies. In order to capture the risk-aversion, we consider the *linear-quadratic* model, i.e., we maximize our expected returns while penalizing for the corresponding quadratic variations:

$$J_T(\dot{\varphi}) = \frac{1}{T} \mathbb{E} \left[\int_0^T \left(\varphi_t \mu_t - \frac{\gamma}{2} (\sigma_t \varphi_t + \xi_t)^2 - \lambda_t G(\dot{\varphi}_t) \right) dt \right]. \quad (2.3)$$

As studied in [19, 24, 51], we trade off expected returns against the tracking error relative to the exogenous target position $-\xi/\sigma$. We can also consider more sophisticated preferences such as exponential or power utility. Notice that the deep reinforcement learning algorithms such as deep hedging, can be easily generalized to sophisticated preferences or utility functions, but the usage of FBSDE solvers is limited since there might not exist a FBSDE system to describe the optimal solution of the hedging problem. See Section 3.3 for details.

To make sure all terms are well defined, we focus on *admissible* strategies that satisfy the same integrability condition $\varphi\sigma \in \mathbb{H}^2$ as in the frictionless case, and whose expected transaction costs are finite:

$$E \left[\int_0^T \lambda_t G(\dot{\varphi}_t) dt \right] < \infty. \quad (2.4)$$

Moreover, we impose the transversality condition to exclude Ponzi scheme:

$$\lim_{\sqrt{\lambda}/T \rightarrow 0} \frac{\lambda}{T^2} \mathbb{E} [\Lambda_T \sigma_T^2 \varphi_T^2] = 0. \quad (2.5)$$

By strict convexity of the goal functional (2.3), optimality of a trading rate $\dot{\varphi}$ is equivalent to the first-order condition that the Gateaux derivative $\lim_{\rho \rightarrow 0} (J_T(\dot{\varphi} + \rho \dot{\eta}) - J_T(\dot{\varphi})) / \rho$ vanishes for *any* admissible perturbation η , cf. [23]:

$$0 = \mathbb{E}_t \left[\int_0^T \left(\mu_t \int_0^t \dot{\eta}_u du - \gamma (\sigma_u \varphi_u + \xi_u) \sigma_u \int_0^t \dot{\eta}_u du - \lambda_t G'(\dot{\varphi}_t) \dot{\eta}_t \right) dt \right].$$

As in [9], this can be rewritten using Fubini's theorem as

$$0 = \mathbb{E}_t \left[\int_0^T \left(\int_t^T (\mu_u - \gamma (\sigma_u \varphi_u + \xi_u) \sigma_u) du - \lambda_t G'(\dot{\varphi}_t) \right) \dot{\eta}_t dt \right].$$

Since this has to hold for *any* perturbation $\dot{\eta}_t$, the tower property of conditional expectation yields

$$\lambda_t G'(\dot{\varphi}_t) = \mathbb{E}_t \left[\int_t^T (\mu_u - \gamma (\sigma_u \varphi_u + \xi_u) \sigma_u) du \right] = M_t + \int_0^t (\gamma (\sigma_u \varphi_u + \xi_u) \sigma_u - \mu_u) du, \quad (2.6)$$

for a martingale $dM_t = Z_t dW_t$ that needs to be determined as part of the solution. Solving for the dynamics of the agents' optimal trading rates would introduce the dynamics of the transaction costs. Accordingly, it is preferable to instead work with the marginal transaction costs transaction costs as the backward process that describes the optimal controls:

$$Y_t := \lambda_t G'(\dot{\varphi}_t), \quad (2.7)$$

and from (2.6) we can infer that $Y_T = 0$. With this notation, the corresponding trading rates are

$$\dot{\varphi}_t = (G')^{-1} \left(\frac{Y_t}{\lambda_t} \right).$$

Thus, the optimal position φ and the corresponding marginal transaction costs Y in turn solve the nonlinear FBSDE

$$d\varphi_t = (G')^{-1} \left(\frac{Y_t}{\lambda_t} \right) dt, \quad \varphi_0 = \varphi_{0-}, \quad (2.8)$$

$$dY_t = (\gamma(\sigma_t\varphi_t + \xi_t)\sigma_t - \mu_t)dt + Z_t dW_t, \quad Y_T = 0. \quad (2.9)$$

For constant quadratic costs $\lambda x^2/2$ and constant volatility σ , this FBSDE becomes linear and can in turn be solved by reducing it to a standard Riccati equation system [9, 13, 46]. For volatilities and quadratic costs that fluctuate randomly, these ODEs are replaced by a backward *stochastic* Riccati equation, compare [8, 41]. With nonlinear costs, no such simplifications are possible. In fact, the wellposedness of the system is generally unclear even for short time horizons since no Lipschitz condition for $(G')^{-1}$ is satisfied.

Reparametrization. In the frictionless analogue of (2.3), pointwise maximization yields the agents' individually optimal strategies, i.e.,

$$\bar{\varphi}_t = \frac{\mu_t}{\gamma\sigma_t^2} - \frac{\xi_t}{\sigma_t}, \quad t \in [0, T]. \quad (2.10)$$

In particular, we can write the dynamic of the frictionless strategy as

$$d\bar{\varphi}_t = \bar{b}_t dt + \bar{a}_t dW_t. \quad (2.11)$$

In real-world applications, people are more interested in the changes induced by transaction costs relative to the frictionless version of the model. To facilitate both the numerical and the analytical analysis, we define

$$\Delta\varphi_t := \varphi_t - \bar{\varphi}_t \quad (2.12)$$

for the difference between the frictional and frictionless positions, which we expect to vanish as the transaction costs tend to zero. In view of the dynamic (2.11) strategy $\bar{\varphi}$ in the frictionless market and the forward equation (2.8), this process has dynamics

$$d\Delta\varphi_t = \left((G')^{-1} \left(\frac{Y_t}{\lambda_t} \right) - \bar{b}_t \right) dt - \bar{a}_t dW_t, \quad \Delta\varphi_0 = \varphi_{0-} + \frac{\xi_0}{\sigma_0} - \frac{\mu_0}{\gamma\sigma_0^2}. \quad (2.13)$$

Accordingly, plugging (2.10) into (2.9), the backward process Y therefore becomes

$$dY_t = \gamma\sigma_t^2 \Delta\varphi_t dt + Z_t dW_t, \quad Y_T = 0. \quad (2.14)$$

Remark 2.2. The analysis is focused on the optimal marginal transaction costs Y instead of the optimal trading rates φ , to avoid the potential extra requirement on the differentiability of $(G')^{-1}$. Moreover, this choice of backward component has linear dynamics, and absorb all the nonlinearity into the dynamic of the forward component, which makes our asymptotic analysis much easier and the numerical solution much more stable.

We choose the deviation of the frictional position with respect to its frictionless counter party as the forward variable, since it exactly is the “fast” variable in the theoretical study in the single agent problem as in [9, 45, 54]. Empirically this choice performs the best in FBSDE solver. Notice that the drift \bar{b} for the frictionless strategy is usually neglected in the small-costs regime, and the frictionless volatility \bar{a} makes the FBSDE system non-deterministic.

3 Deep Learning-based Numerical Algorithms

For practitioners, it is crucial to get the optimal trading strategy numerically, in a time-efficient manner, hence efficient numerical methods to solve the optimization problem (2.3) are in need. With the development of GPUs and highly accurate machine learning models, the optimal hedging problems can be solved numerically by using learning-based algorithms. There are two numerical approaches to do so: numerically solving the FBSDE system (2.13) - (2.14) or directly targeting the goal functional (2.3). In this section, we present two deep learning-based numerical algorithms guided by these ideas.

A natural idea to start with is to solve the associated FBSDE system (2.13) - (2.14) numerically. Since the dimension of the FBSDEs grows quickly with the number of assets and agents, and the boundary conditions are unclear, classical numerical methods such as finite differences fail to work. However, the learning-based algorithms can bypass the need to identify the correct boundary conditions and overcome the curse of dimensionality. The first learning-based introduced in Section 3.1 is the FBSDE solver, proposed in the spirit of the BSDE approach by Han, Jentzen, and E in [32]. The algorithm approximates the dependence of the backward components on the forward components by a deep neural network, and it solves the FBSDE through simulation and stochastic gradient descent methods. It can also handle higher-dimensional settings, e.g., random and time-varying transaction costs, returns, and volatility processes. In addition, the FBSDE solver can even solve equilibrium models as is used in [26]. FBSDE solver works very well when the time horizon is not too long, and the convergence of this method with respect to a special class of FBSDE systems is established in small time durations in [33]. However, the FBSDE solver does not scale well when the trading horizon or time discretization is large. In our example, with calibrated market parameters from [26], the FBSDE solver fails to converge if we consider a more than one trading year trading horizon (approximately 252 trading days). Furthermore, in some complicated cases, we cannot even characterize the optimal trading problem with a system of FBSDEs.

In order to overcome the difficulties mentioned above, we consider deep reinforcement learning framework that is known as deep hedging in Section 3.2. The name for this type of algorithms comes from the groundbreaking *Deep Hedging* work of Buehler et.al. [14, 15]. Pioneered by [12, 34, 36, 37, 44, 47, 48, 49, 50], various reinforcement learning algorithms are implemented and perform extreme success in portfolio optimization problems with transaction costs. Reinforcement learning can even solve the Nash equilibria, see [16] for details. The key idea is to directly parametrize the optimal trading rate and optimize the discretized version of preference (2.3). Then, through stochastic gradient descent based algorithms and back-propagation, the reinforcement algorithm updates the parameters of the networks until a (local) optimizer is found (see [55] for a detailed introduction). However, deep hedging algorithms require a huge number of simulated sample paths and finer discretization of the trading time horizon, which makes the training time significantly longer than FBSDE solver.

The organization of the rest of the section is as follows. First, we introduce the FBSDE solver in Section 3.1 and the deep hedging algorithm in Section 3.2. We implement both of the algorithms and test them on various models which even includes more than one stocks and/or with stochastic liquidity risk, and we discuss and document their advantages and disadvantages in these empirical implementations in Section 3.3.

3.1 FBSDE Solver

Let us describe the algorithm in more detail. The key observation is that the dynamic of the system (2.13) - (2.14) is pinned down if the volatility Z of the backward component Y is specified.

Indeed, let us fix a time partition $0 = t_0 < \dots < t_N = T$, where $t_m = mT/N$ and $\Delta t = T/N$. Let $(\Delta W_m)_{m=0}^N$ be iid normally distributed random variables with mean zero and variance Δt . At time t_m , we have μ_{t_m} , σ_{t_m} and λ_{t_m} from the market and the endowment volatility ξ_{t_m} , the drift \bar{b}_{t_m} and volatility \bar{a}_{t_m} for the frictionless strategy of the agent. With $(\Delta W_m, \Delta\varphi_{t_m})$ as input for each time step, the discrete-time analogue of the forward update rule for the FBSDE system (2.13) - (2.14) becomes

$$\Delta\varphi_{t_{m+1}} = \Delta\varphi_{t_m} + \left((G')^{-1} \begin{pmatrix} Y_{t_m} \\ \lambda_{t_m} \end{pmatrix} - \bar{b}_{t_m} \right) \Delta t - \bar{a}_{t_m} \Delta W_m, \quad (3.1)$$

$$Y_{t_{m+1}} = Y_{t_m} + \gamma\sigma_{t_m}^2 \Delta\varphi_{t_m} \Delta t + Z_{t_m} \Delta W_m. \quad (3.2)$$

Together with a guess for the initial values of the backward components, we can then simulate the system with a standard forward scheme and check whether it satisfies the terminal condition as $Y_T = 0$. Searching for the correct initial values is relatively straightforward. The more difficult challenge is parametrizing the “controls” Z – which are functions of time and the forward processes – and updating the corresponding initial guesses until the terminal condition is matched sufficiently well. In [32], Han, Jentzen, and E introduced the innovative way to parametrize Z . At each time point t_m , they parametrized Z_{t_m} with a (shallow) network structure F^{θ_m} , with time t_m value of the forward components as the inputs. Together with the guess of the initial value of the backward component, which we denote as Y_0^θ , the system can then be simulated forward in time. In this way, the shallow network structures are concatenated over time and become a deep neural network architecture, since the number of layers of the architecture and the number of parameters in the networks grows linearly in the number of discretization steps N . In other words, we input simulated Brownian paths into the deep network structure, and it outputs the terminal values of the backward components.

Our task is to update the parameters $\{Y_0^\theta, \theta_m, m = 0, \dots, N\}$ until the terminal conditions $Y_T = 0$ are matched sufficiently well. This iterative update of the network parameters until $Y_T = 0$ is the essence of *supervised machine learning* tasks. State-of-the-art performance is achieved through back-propagation and stochastic gradient descent-type algorithms, see [27] for more details.

Remark 3.1. Recall that there is no assumption on the dynamic of the market. Here, however, we need to mildly assume that we can simulate the return μ and volatilities σ , the drift \bar{b} and volatilities \bar{a} for the frictionless position $\bar{\varphi}$ from (2.11), as well as the endowment volatilities ξ .

Now, we focus on the parametrization of $\{Z_{t_m}\}_{m=0}^N$ within a function class $\{F^\theta : \theta \in \Theta\}$. A very popular class of functions in the machine learning community is the “singular activation function Rectified Linear Unit” (*ReLU*): $ReLU(x) = \max\{x, 0\}$. A popular class of approximation function F is the convolution of linear functions with *ReLU* activations. For the numerical experiments in Section 4, at each time t_m , the F^{θ_m} we use is a neural network with one hidden layer of 15 hidden units with batch normalization (BN), and that is

$$F^{\theta_m}(x) = w_{\theta_m}^2 \left(ReLu \left(BN \left(w_{\theta_m}^1 x + b_{\theta_m}^1 \right) \right) \right) + b_{\theta_m}^2.$$

Recall that with the Brownian motion W as a 1-dim process, and the forward component φ as a 1-dim vector, Z is also a 1-dim vector. $w_{\theta_m}^1 \in \mathbb{R}^{15 \times 2}$ and $b_{\theta_m}^1 \in \mathbb{R}^{15}$ are called the input *weights* and *biases* of the network, whereas $w_{\theta_m}^2 \in \mathbb{R}^{1 \times 15}$ and $b_{\theta_m}^2 \in \mathbb{R}^1$ are called the output *weights* and *biases* of the network. We summarize the structure of FBSDE solver in Algorithm 1:

Algorithm 1: Training Procedure of FBSDE Solver

Data: $\Delta\varphi_{t_0}^\theta = \varphi_{0-} + \frac{\xi_0}{\sigma_0} - \frac{\mu_0}{\gamma\sigma_0^2}$, $W_{t_0} = 0$, γ , dynamic of processes μ , σ , λ , ξ , \bar{b} and \bar{a} ;

- 1 initialization of parameters $\{Y_0^\theta, \theta_m, m = 0, \dots, N\}$, $m = 0$, $Y_{t_0}^\theta = Y_0^\theta$;
- 2 **while** $epoch \leq Epoch$ **do**
- 3 sample ΔW , `batch_size` $\times N$ iid Gaussian random variables with variance Δt ;
- 4 **while** $m < N$ **do**
- 5 $Z_{t_m}^\theta = F^{\theta_m}(W_{t_m}, \Delta\varphi_{t_m}^\theta)$;
- 6 $Y_{t_{m+1}}^\theta = Y_{t_m}^\theta + \gamma\sigma_{t_m}^2 \Delta\varphi_{t_m}^\theta \Delta t + Z_{t_m}^\theta \Delta W_m$;
- 7 $\Delta\varphi_{t_{m+1}}^\theta = \Delta\varphi_{t_m}^\theta + (G')^{-1} \left(\frac{Y_{t_m}^\theta}{\lambda_{t_m}} \right) \Delta t - \bar{b}_{t_m} \Delta t - \bar{a}_{t_m} \Delta W_m$;
- 8 $W_{t_{m+1}} = W_{t_m} + \Delta W_m$;
- 9 $m++$;
- 10 **end**
- 11 Output $Y_T^\theta = Y_{t_N}^\theta$;
- 12 Loss = $\|Y_T^\theta\|^2 / \text{batch_size}$;
- 13 Calculate the gradient of Loss with respect to θ ;
- 14 Back propagate updates for $\{Y_0^\theta, \theta_m, m = 0, \dots, N\}$ via Adam;
- 15 epoch ++;
- 16 **end**
- 17 **return:** (local) optimizer $\theta^* = \{Y_0^{\theta^*}, \theta_m^*, m = 0, \dots, N\}$.

3.2 Deep Hedging Networks

Let us fix a time partition $0 = t_0 < \dots < t_N = T$, where $t_m = mT/N$ and $\Delta t = T/N$. Under this partition, for a single simulation, the discretized version of the goal functional (2.3), becomes

$$J_T(\dot{\varphi}) = \frac{1}{N} \sum_{m=0}^{N-1} \left[\varphi_{t_m} \mu_{t_m} - \frac{\gamma}{2} (\sigma_{t_m} \varphi_{t_m} + \xi_{t_m})^2 - \lambda_{t_m} G(\dot{\varphi}_{t_m}) \right], \quad (3.3)$$

where φ follows the discretized version of update process

$$\varphi_{t_{m+1}} = \varphi_{0-} + \sum_{k=0}^m \dot{\varphi}_{t_k} \Delta t = \varphi_{t_m} + \dot{\varphi}_{t_m} \Delta t.$$

At each time point t_m , we directly parametrize the trading strategy $\dot{\varphi}_{t_m}$ using a (comparatively shallow) network F^{θ_m} . For the numerical experiments in Section 4, the neural network we use has three hidden layers with 10, 15 and 10 hidden units, respectively. We also implement the batch normalization (BN) at each hidden layer and that is, for $l = 1, 2, 3$:

$$F^{\theta_m}(x) = w_{\theta_m}^4 \left(F_3^{\theta_m} \left(F_2^{\theta_m} \left(F_1^{\theta_m}(x) \right) \right) \right) + b_{\theta_m}^4, \quad F_l^{\theta_m}(x) = \text{ReLu} \left(\text{BN} \left(w_{\theta_m}^l x + b_{\theta_m}^l \right) \right).$$

Recall that with time t as a real number, the Brownian motion W as a 1-dim process, and the forward component φ as a 1-dim vector, $\dot{\varphi}$ is also a 1-dim vector. $w_{\theta_m}^1 \in \mathbb{R}^{10 \times 3}$ and $b_{\theta_m}^1 \in \mathbb{R}^{10}$ are called the input *weights* and *biases* of the network, and $w_{\theta_m}^2 \in \mathbb{R}^{15 \times 10}$, $b_{\theta_m}^2 \in \mathbb{R}^{15}$, $w_{\theta_m}^3 \in \mathbb{R}^{10 \times 15}$ and $b_{\theta_m}^3 \in \mathbb{R}^{10}$ are called the hidden *weights* and *biases*, whereas $w_{\theta_m}^4 \in \mathbb{R}^{1 \times 10}$ and $b_{\theta_m}^4 \in \mathbb{R}^1$ are called the output *weights* and *biases* of the network. We summarize the deep hedging algorithm in Algorithm 2 as follows:

Algorithm 2: Training Procedure of Deep Hedging Algorithm

Data: $\varphi_{t_0}^\theta = \varphi_{0-}$, $W_{t_0} = 0$, γ , dynamic of processes μ , σ , λ and ξ

- 1 initialization of parameters $\{\theta_m, m = 0, \dots, N\}$, $m = 0$;
- 2 **while** $epoch \leq Epoch$ **do**
- 3 sample ΔW , $batch_size \times N \times d$ iid Gaussian random variables with variance Δt ;
- 4 **while** $m < N$ **do**
- 5 $\dot{\varphi}_{t_m}^\theta = F^{\theta_m}(t_m, W_{t_m}, \varphi_{t_m}^\theta)$;
- 6 $\varphi_{t_{m+1}}^\theta = \dot{\varphi}_{t_m}^\theta \Delta t + \varphi_{t_m}^\theta$;
- 7 $W_{t_{m+1}} = W_{t_m} + \Delta W_m$;
- 8 $m++$;
- 9 **end**
- 10 $Loss = -\sum_{m=0}^N [\varphi_{t_m}^\theta \mu_{t_m} - \frac{\gamma}{2} (\sigma_{t_m} \varphi_{t_m}^\theta + \xi_{t_m})^2 - \lambda_{t_m} G(\dot{\varphi}_{t_m}^\theta)] / (N \times batch_size)$;
- 11 Calculate the gradient of $Loss$ with respect to θ ;
- 12 Back propagate updates for $\{\theta_m, m = 0, \dots, N\}$ via Adam (switch to SGD when fine tuning);
- 13 $epoch++$;
- 14 **end**
- 15 **return:** (local) optimizer $\theta^* = \{\theta_m^*, m = 0, \dots, N\}$

3.3 Comparison of FBSDE Solver and Deep Hedging Algorithms

After introducing the optimal hedging problem with market frictions as (2.3), we implement the FBSDE solver and deep hedging algorithm and test them in various market settings. The details and codes are available here: <https://github.com/InnerPeas/ML-for-Transaction-Costs>.

Empirically, the appearance of the extreme value in the dynamic of the FBSDE solver may affect the calculation precision and thus jeopardize the performance. In particular, the performance and the harness of tuning of the FBSDE solvers becomes significantly worse if we increase the number of forward and backward variables in the FBSDE system with respect to multiple stocks settings. In comparison, the deep hedging still works well, which shows good scalability with respect to the increase of dimensions.

A major drawback of both algorithm is when the trading time horizon is too long, both of the algorithms fail to converge. Even in the intermediate trading time horizon when the deep hedging algorithm still works, it requires significant training time even for experienced programmers. On the other hand, the leading-order asymptotic optimal strategy $\dot{\varphi} = (\dot{\varphi}_t)_{t \in [0, T]}$ for the frictional mean-variance preference (2.3) is available, namely, (with a little abuse of notation),

$$\dot{\varphi}_t = -\text{sign}(\varphi_t - \bar{\varphi}_t) \times (G')^{-1} \left(\frac{g(|\varphi_t - \bar{\varphi}_t|; \gamma, \sigma_t, \bar{a}_t, \lambda_t)}{\lambda_t} \right), \quad (3.4)$$

where g is the unique solution to the following ODE with proper ‘‘mean-reverting’’ requirement:

$$(G')^{-1} \left(\frac{g(x; \gamma, \sigma, \bar{a}, \lambda)}{\lambda} \right) g'(x; \gamma, \sigma, \bar{a}, \lambda) + \frac{\bar{a}^2}{2} g''(x; \gamma, \sigma, \bar{a}, \lambda) = \gamma \sigma^2 x. \quad (3.5)$$

This leading-order formula (3.4) and the associated ODE (3.5) are proposed and studied formally in [10, 18, 31, 40, 54], and we refer the readers to Appendix A for details of the derivation and rigorous proof in a special case. Notice that once we obtain the numerical solution of (3.5), the leading-order formula can be applied *immediately*. In Section 4, we compare the performances

of numerical algorithms together with the leading-order approximations, to have a better idea of when to use which methods. Based on the experiment results in Section 4, we propose a “pasting” algorithm, in order to increase the scalability of deep learning-based algorithms with respect to time horizon.

We summarize the our empirical observations (High/Medium/Low or Yes/No) in the following table:

	FBSDE Solver	Deep Hedging
Scalability wrt time	Low	Medium
Scalability wrt dimension	Medium	High
Convergence speed	High (if algorithm converges)	Medium
Hardness of tuning	Low (if algorithm converges)	Medium
Sensitivity to calculation precision	High	Medium
Multiple stocks	Yes	Yes
General utility functions	Limited	Yes
General market dynamics	Yes	Yes

4 Experiments and Comparison Results

In this section, the FBSDE solver algorithms described in 3.1 and the deep hedging algorithm described in 3.2 are implemented. To illustrate the performance of the FBSDE solver and the deep hedging algorithm, we consider two calibrated Bachelier models without liquidity risk: a quadratic transaction costs model, and a general power costs model with elastic parameter $q = 3/2$. In all experiments, the parameters are from the calibration of real-world time series data in [26]. The agent’s risk aversion is set to be $\gamma = 1.66 \times 10^{-13}$, the total shares outstanding in the market is $s = 2.46 \times 10^{11}$, and the stock return is $\mu = \frac{1}{2}\gamma\sigma^2s$ with the stock volatility being $\sigma = 1.88^1$. The implementation details and codes can be found here: <https://github.com/InnerPeas/ML-for-Transaction-Costs/blob/main/README.md>.

4.1 Quadratic Transaction Costs $G(x) = x^2/2$.

With $G(x) = x^2/2$, on top of the leading-order approximation, the FBSDE system (2.13) - (2.14) becomes linear and the optimal trading strategy is given explicitly by:

$$\dot{\varphi}_t = -\sqrt{\frac{\gamma\sigma^2}{\lambda}} \tanh\left(\sqrt{\frac{\gamma\sigma^2}{\lambda}}(T-t)\right) \left(\varphi_{0-} + \frac{\xi_0}{\sigma} - \frac{\mu_0}{\gamma\sigma^2} - \int_0^t \frac{\bar{a} dW_u}{\cosh\sqrt{\frac{\gamma\sigma^2}{\lambda}}(T-u)}\right). \quad (4.1)$$

The remaining parameters are taken from the calibrations from Section 5 in [26], where under quadratic costs the endowment volatility parameter $\xi = 2.19 \times 10^{10}$ and the liquidity level parameter is $\lambda = 1.08 \times 10^{-10}$. With the trading horizon $T = 10, 21, 42, 252, 2520$ trading days, the performance of both learning methods and the leading order approximation are summarized in Table 1 - 5 and illustrated in Figure 1 - 5. To account for the large Monte Carlo error from the long trading

¹In [26], calibration is done for an equilibrium model of two agents where the asset returns depend on the risk aversion of both agents. In our single-agent model we just take the asset’s parameters to provide a more realistic numerical analysis. Although the models considered here are Bachelier, it can be generalized to Geometric Brownian motion models and the whole calculation and derivation follow if we switch our current analysis from shares positions to money in stock positions, with the unit of the transaction costs changed accordingly.

horizons such as $T = 2520$ trading days (which is approximately 10 trading years), we evaluated the performance of our models using 100 million sample paths.

When the trading horizon is relatively short ($T \leq 42$ trading days), the performance of the FBSDE solver is the closest to the ground truth path-wisely, see Figure 1 - 3. It means that when the FBSDE solver converges, it can learn the optimal trading strategy perfectly. However, as is already experienced in [26], when the trading horizon is longer than one trading year, the FBSDE solver fails to converge.

On the other hand, the performance of the deep hedging algorithm with intermediate time horizons is better. Especially it can still work well once the hyperparameters are appropriately tuned, whereas the FBSDE solver fails to converge, as illustrated in Figure 4 - 5 and Table 4 - 5. However, we can see that under-fitting phenomena exist, and it becomes more and more severe as the trading horizon increases from $T = 10$ to $T = 2520$ while time discretization $N = 168$ remains the same. To achieve state-of-art performance, we choose the time discretization as $N = 252$ when $T = 252$ and $N = 2520$ when $T = 2520$.

Finally, the performance of the leading-order asymptotic approximation (3.4) becomes better and better as the time horizon becomes longer. From the mean squared error of $\dot{\varphi}_T/s$ in the last column of Table 1 - 5, we can see that shortly around the terminal time, the leading order approximation diverges substantially from 0. This observation is consistent with the figures of $\dot{\varphi}$ and φ as in Figure 1 - 5. In other words, we are giving up the performance at the very end of the trading horizon to get an overall near-optimal performance without spending hours or days on tuning the hyperparameters in the machine learning algorithms. In fact, when the trading horizon is as large as $T = 2520$ trading days, leading order approximation achieves the closest expected utility to the ground truth, while deep hedging is hard to train as the variance of stock price adapted to Brownian motion becomes very large with long trading horizon.

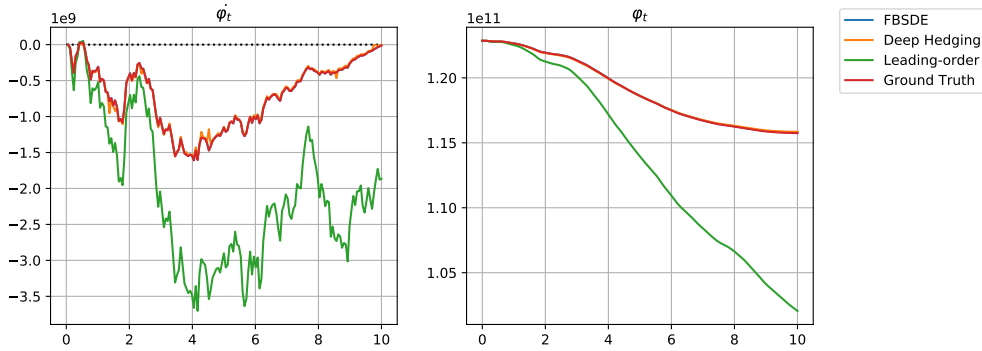


Figure 1: Optimal trading rates $\dot{\varphi}$ (left panel) and optimal positions φ (right panel) for trading horizon $T = 10$ days with calibrated parameters under quadratic costs.

Method (discretization=168)	$J_T(\dot{\varphi}) \pm \text{std}$	$\mathbb{E}[\dot{\varphi}_T ^2/s^2]$
Deep Hedging	$4.24 \times 10^9 \pm 1.54 \times 10^9$	2.63×10^{-10}
FBSDE Solver	$4.24 \times 10^9 \pm 1.54 \times 10^9$	1.99×10^{-9}
Leading Order Approximation	$4.17 \times 10^9 \pm 1.55 \times 10^9$	6.40×10^{-5}
Ground Truth	$4.24 \times 10^9 \pm 1.54 \times 10^9$	1.98×10^{-9}

Table 1: Expectation and standard deviation of preference J_T , and mean squared error of $\dot{\varphi}_T/s$ for trading horizon $T = 10$ days with calibrated parameters under quadratic costs.

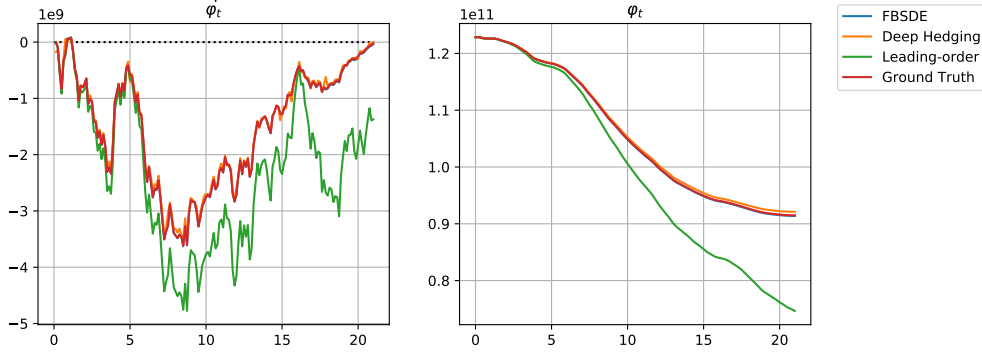


Figure 2: Optimal trading rates $\dot{\varphi}$ (left panel) and optimal positions φ (right panel) for trading horizon $T = 21$ days with calibrated parameters under quadratic costs.

Method (discretization=168)	$J_T(\dot{\varphi}) \pm \text{std}$	$\mathbb{E}[\dot{\varphi}_T ^2/s^2]$
Deep Hedging	$4.11 \times 10^9 \pm 2.23 \times 10^9$	3.29×10^{-9}
FBSDE Solver	$4.11 \times 10^9 \pm 2.24 \times 10^9$	2.72×10^{-8}
Leading Order Approximation	$4.05 \times 10^9 \times 2.24 \times 10^9$	7.98×10^{-5}
Ground Truth	$4.11 \times 10^9 \pm 2.23 \times 10^9$	1.27×10^{-8}

Table 2: Expectation and standard deviation of preference J_T , and mean squared error of $\dot{\varphi}_T/s$ for trading horizon $T = 21$ days with calibrated parameters under quadratic costs.

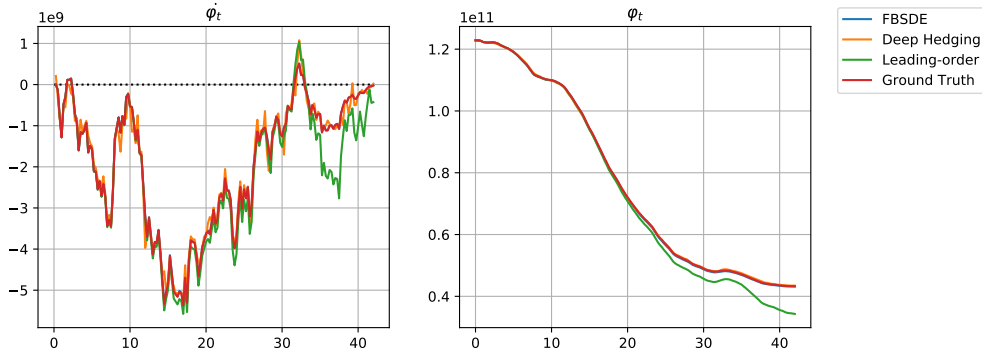


Figure 3: Optimal trading rates $\dot{\varphi}$ (left panel) and optimal positions φ (right panel) for trading horizon $T = 42$ days with calibrated parameters under quadratic costs.

Method (discretization=168)	$J_T(\dot{\varphi}) \pm \text{std}$	$\mathbb{E}[\dot{\varphi}_T ^2/s^2]$
Deep Hedging	$4.00 \times 10^9 \pm 3.15 \times 10^9$	2.33×10^{-7}
FBSDE Solver	$4.00 \times 10^9 \pm 3.15 \times 10^9$	5.53×10^{-8}
Leading Order Approximation	$3.97 \times 10^9 \pm 3.15 \times 10^9$	8.43×10^{-5}
Ground Truth	$4.00 \times 10^9 \pm 3.15 \times 10^9$	5.46×10^{-8}

Table 3: Expectation and standard deviation of preference J_T , and mean squared error of $\dot{\varphi}_T/s$ for trading horizon $T = 42$ days with calibrated parameters under quadratic costs.

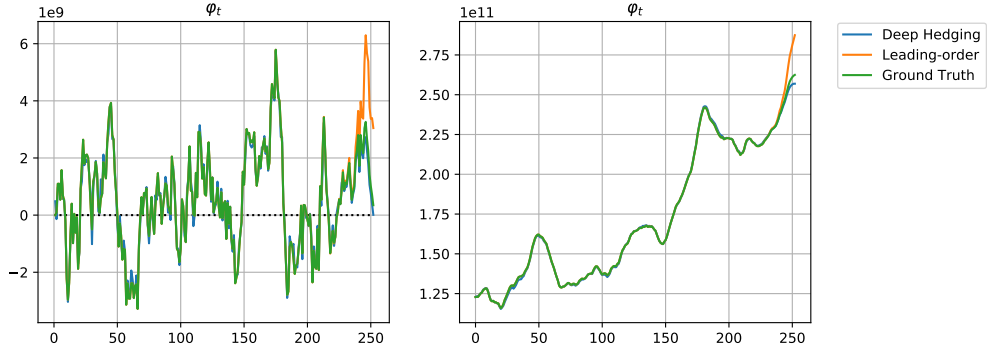


Figure 4: Optimal trading rates $\dot{\varphi}$ (left panel) and optimal positions φ (right panel) for trading horizon $T = 252$ days with calibrated parameters under quadratic costs.

Method (discretization=252)	$J_T(\dot{\varphi}) \pm \text{std}$	$\mathbb{E}[\dot{\varphi}_T ^2/s^2]$
Deep Hedging	$3.88 \times 10^9 \pm 7.68 \times 10^9$	7.01×10^{-8}
FBSDE Solver	NaN	NaN
Leading Order Approximation	$3.86 \times 10^9 \pm 7.68 \times 10^9$	8.92×10^{-5}
Ground Truth	$3.87 \times 10^9 \pm 7.68 \times 10^9$	8.16×10^{-7}

Table 4: Expectation and standard deviation of preference J_T , and mean squared error of $\dot{\varphi}_T/s$ for trading horizon $T = 252$ days with calibrated parameters under quadratic costs.

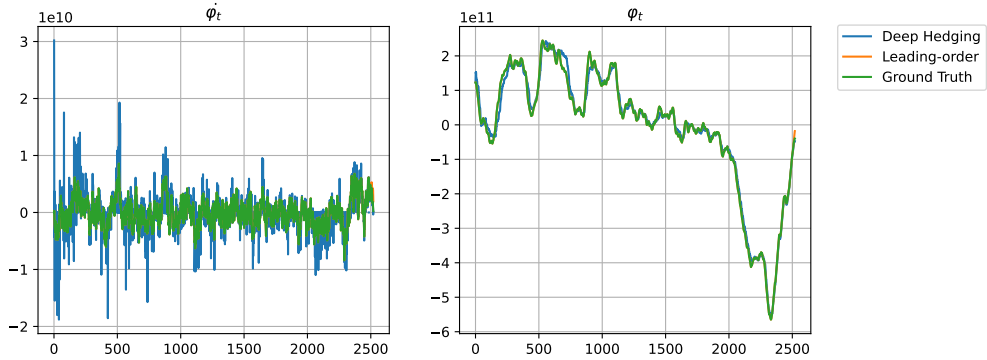


Figure 5: Optimal trading rates $\dot{\varphi}$ (left panel) and optimal positions φ (right panel) for trading horizon $T = 2520$ days with calibrated parameters under quadratic costs.

Method (discretization=2520)	$J_T(\dot{\varphi}) \pm \text{std}$	$\mathbb{E}[\dot{\varphi}_T ^2/s^2]$
Deep Hedging	$3.43 \times 10^9 \pm 2.43 \times 10^{10}$	5.61×10^{-9}
FBSDE Solver	NaN	NaN
Leading Order Approximation	$3.85 \times 10^9 \pm 2.43 \times 10^{10}$	8.91×10^{-5}
Ground Truth	$3.85 \times 10^9 \pm 2.43 \times 10^{10}$	8.16×10^{-7}

Table 5: Expectation and standard deviation of preference J_T , and mean squared error of $\dot{\varphi}_T/s$ for trading horizon $T = 2520$ days with calibrated parameters under quadratic costs.

4.2 Power Transaction Costs $G(x) = |x|^q/q$ with $q=3/2$.

The analogous experiments for power costs with $q = 3/2$ are also done with calibrated parameters from Section 5 in [26], where the endowment volatility is $\xi_{1.5} = 2.33 \times 10^{10}$ and liquidity level $\lambda_{1.5} = 5.22 \times 10^{-6}$. In the general superlinear power transaction costs case, i.e. $G(x) = |x|^q/q$ with $q \in (1, 2)$, the ground truth is no longer available in closed form. Nevertheless, we can still compare the numerical results from the machine learning algorithms and our leading order asymptotic results. The models are evaluated using 100 million sample paths in order to account for the large Monte Carlo error from long trading horizons.

With the dynamics of the system being nonlinear, the FBSDE solver converges on shorter trading horizons, i.e., $T < 21$ trading days, shown in Figure 6 - 7 and Table 6 - 7. When the trading horizon is large, i.e., $T \geq 42$ days, the FBSDE solver fails to converge. The deep hedging algorithm obtains similar results as the FBSDE solver with short time horizons, as shown in Figure 6 - 7 and Table 6 - 7. With longer time horizons, the deep heading algorithm can still work when the FBSDE solver fails to converge, see Figure 8 - 10 and Table 8 - 10. Similar as in the quadratic costs case, as the trading horizon increases, the performance of the leading order approximation is getting closer to the optimal results learnt by the machine learning algorithm, which justifies the approximation result of the leading-order approximation (3.4) empirically. On the contrary, when the trading horizon is as long as 10 trading years, deep hedging becomes suboptimal because of the large variance from sample paths of Brownian motion.

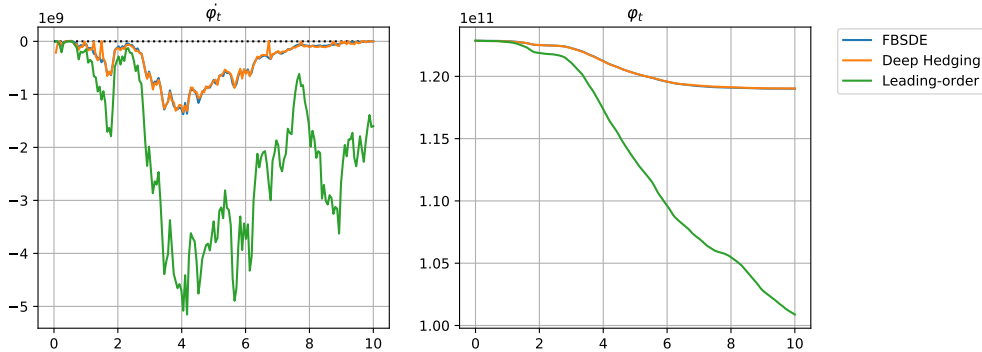


Figure 6: Optimal trading rates $\dot{\varphi}$ (left panel) and optimal positions φ (right panel) for trading horizon $T = 10$ days with calibrated parameters under $q = 3/2$ costs.

Method (discretization=168)	$J_T(\dot{\varphi}) \pm \text{std}$	$\mathbb{E}[\dot{\varphi}_T ^2/s^2]$
Deep Hedging	$4.21 \times 10^9 \pm 1.67 \times 10^9$	3.22×10^{-10}
FBSDE Solver	$4.21 \times 10^9 \pm 1.67 \times 10^9$	1.72×10^{-10}
Leading Order Approximation	$4.10 \times 10^9 \pm 2.00 \times 10^9$	9.01×10^{-5}

Table 6: Expectation and standard deviation of preference J_T , and mean squared error of $\dot{\varphi}_T/s$ for trading horizon $T = 10$ days with calibrated parameters under $q = 3/2$ costs.

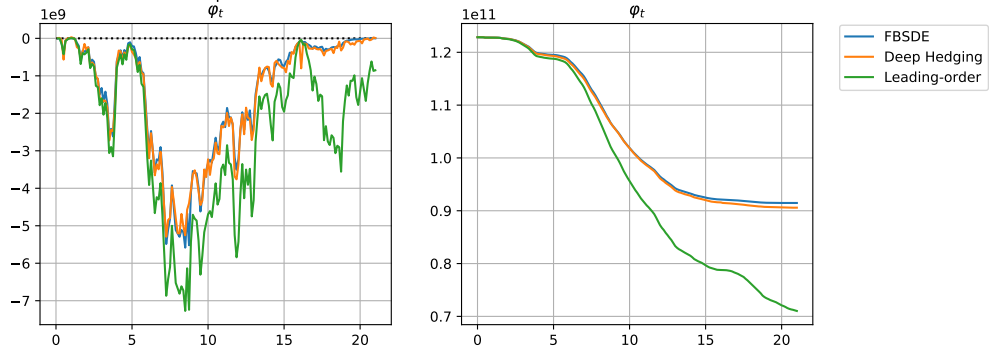


Figure 7: Optimal trading rates $\dot{\varphi}$ (left panel) and optimal positions φ (right panel) for trading horizon $T = 21$ days with calibrated parameters under $q = 3/2$ costs.

Method (discretization=168)	$J_T(\dot{\varphi}) \pm \text{std}$	$\mathbb{E}[\dot{\varphi}_T ^2/s^2]$
Deep Hedging	$4.04 \times 10^9 \pm 2.52 \times 10^9$	1.99×10^{-9}
FBSDE Solver	$4.04 \times 10^9 \pm 2.51 \times 10^9$	6.37×10^{-9}
Leading Order Approximation	$3.96 \times 10^9 \pm 2.73 \times 10^9$	1.11×10^{-4}

Table 7: Expectation and standard deviation of preference J_T , and mean squared error of $\dot{\varphi}_T/s$ for trading horizon $T = 21$ days with calibrated parameters under $q = 3/2$ costs.

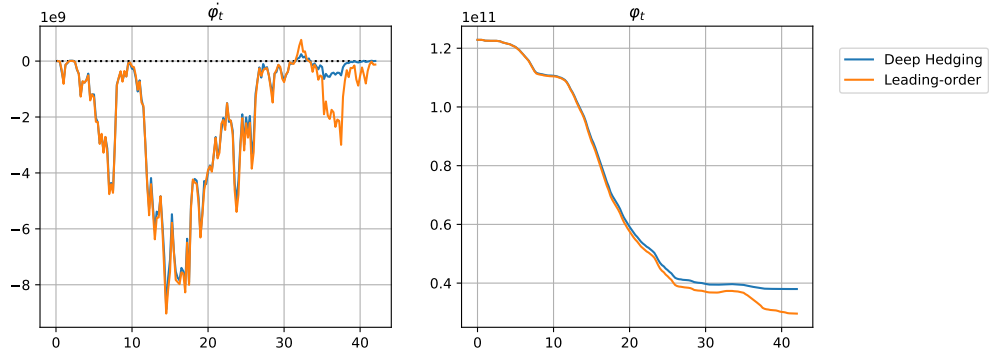


Figure 8: Optimal trading rates $\dot{\varphi}$ (left panel) and optimal positions φ (right panel) for trading horizon $T = 42$ days with calibrated parameters under $q = 3/2$ costs.

Method (discretization=168)	$J_T(\dot{\varphi}) \pm \text{std}$	$\mathbb{E}[\dot{\varphi}_T ^2/s^2]$
Deep Hedging	$3.92 \times 10^9 \pm 3.56 \times 10^9$	1.39×10^{-8}
FBSDE Solver	NaN	NaN
Leading Order Approximation	$3.87 \times 10^9 \pm 3.65 \times 10^9$	1.15×10^{-4}

Table 8: Expectation and standard deviation of preference J_T , and mean squared error of $\dot{\varphi}_T/s$ for trading horizon $T = 42$ days with calibrated parameters under $q = 3/2$ costs.

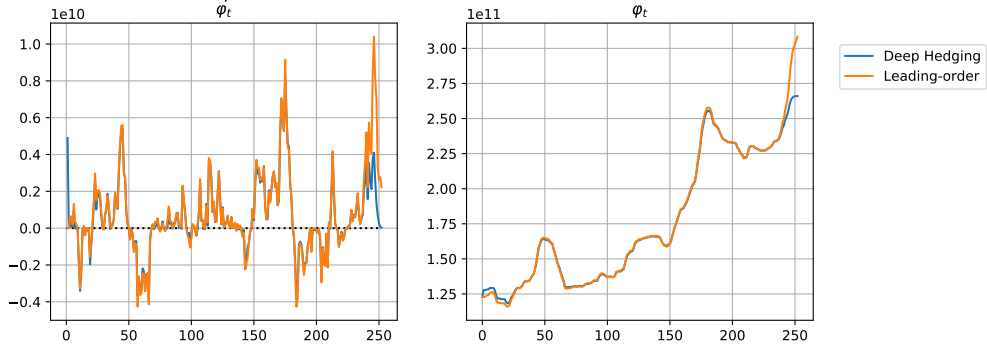


Figure 9: Optimal trading rates $\dot{\varphi}$ (left panel) and optimal positions φ (right panel) for trading horizon $T = 252$ days with calibrated parameters under $q = 3/2$ costs.

Method (discretization=252)	$J_T(\dot{\varphi}) \pm \text{std}$	$\mathbb{E}[\dot{\varphi}_T ^2/s^2]$
Deep Hedging	$3.78 \times 10^9 \pm 8.31 \times 10^9$	9.27×10^{-9}
FBSDE Solver	NaN	NaN
Leading Order Approximation	$3.78 \times 10^9 \pm 8.32 \times 10^9$	1.2×10^{-4}

Table 9: Expectation and standard deviation of preference J_T , and mean squared error of $\dot{\varphi}_T/s$ for trading horizon $T = 252$ days with calibrated parameters under $q = 3/2$ costs.

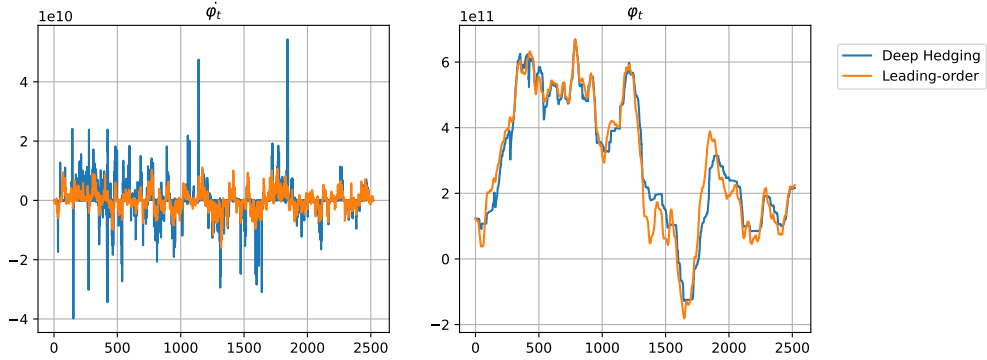


Figure 10: Optimal trading rates $\dot{\varphi}$ (left panel) and optimal positions φ (right panel) for trading horizon $T = 2520$ days with calibrated parameters under $q = 3/2$ costs.

Method (discretization=2520)	$J_T(\dot{\varphi}) \pm \text{std}$	$\mathbb{E}[\dot{\varphi}_T ^2/s^2]$
Deep Hedging	$3.31 \times 10^9 \pm 2.60 \times 10^{10}$	8.71×10^{-8}
FBSDE Solver	NaN	NaN
Leading Order Approximation	$3.78 \times 10^9 \pm 2.59 \times 10^{10}$	1.2×10^{-4}

Table 10: Expectation and standard deviation of preference J_T , and mean squared error of $\dot{\varphi}_T/s$ for trading horizon $T = 2520$ days with calibrated parameters under $q = 3/2$ costs.

4.3 Pasting Algorithms

The optimal hedging problem can be treated in two folds. On the numerical aspect, as the development of deep-learning based algorithm, we can also solve the system through various different scheme, which is discussed in details in Section 3. On the theoretical aspect, one can study the *asymptotic* limiting behavior as the trading horizon T goes to ∞ . A natural following question is, when the trading horizon T is identified as long and whether it is related to the smallness assumption of the transaction costs level λ . It turns out, in the Bachelier models without liquidity risk, the ‘‘magic’’ quantity is $\sqrt{\lambda}/T$; namely, the smallness assumption of λ and the definition of long trading horizon are both relative quantities, depending on whether $\sqrt{\lambda}/T$ is of higher order of 1. Even more surprisingly, $O(\sqrt{\lambda}/T)$ is the approximation accuracy for the leading-order approximation (3.4), that is independent of the choice of the transaction costs.

Therefore, we propose the following algorithm to take advantage of the leading-order approximation formula (3.4), in order to increase the scalability of deep learning-based algorithm with respect to the trading horizon as well as reduce the training time:

Algorithm 3: Training Procedure of Pasting Algorithm with Deep Hedging	
<p>Data: $\Delta\varphi_{t_0}^\theta = \varphi_{0-} + \frac{\xi_0}{\sigma_0} - \frac{\mu_0}{\gamma\sigma_0^2}$, $W_{t_0} = 0$, γ, κ, λ, dynamic of processes $\mu, \sigma, \Lambda, \xi, \bar{\varphi}, \bar{a}$;</p>	
1	$M = \min \left\{ m : T - t_m < \kappa\sqrt{\lambda} \right\}$, $m = 0$;
2	while $epoch \leq Epoch$ do
3	sample ΔW , <code>batch_size</code> $\times N$ iid Gaussian random variables with variance Δt ;
4	while $m < M$ do
5	$\varphi_{t_{m+1}}^\theta = \varphi_{t_m}^\theta - \text{sign}(\varphi_{t_m}^\theta - \bar{\varphi}_{t_m}) \times (G')^{-1} \left(\frac{g(\varphi_{t_m}^\theta - \bar{\varphi}_{t_m} ; \gamma, \sigma_{t_m}, \bar{a}_{t_m}, \lambda\Lambda_{t_m})}{\lambda\Lambda_{t_m}} \right) \Delta t$;
6	$W_{t_{m+1}} = W_{t_m} + \Delta W_m$;
7	$m++$;
8	end
9	while $m < N$ do
10	$\dot{\varphi}_{t_m}^\theta = F^{\theta_m}(t_m, W_{t_m}, \varphi_{t_m}^\theta)$;
11	$\varphi_{t_{m+1}}^\theta = \dot{\varphi}_{t_m}^\theta \Delta t + \varphi_{t_m}^\theta$;
12	$W_{t_{m+1}} = W_{t_m} + \Delta W_m$;
13	$m++$;
14	end
15	$Loss = -\sum_{m=0}^N \left[\varphi_{t_m}^\theta \mu_{t_m} - \frac{\gamma}{2} (\sigma_{t_m} \varphi_{t_m}^\theta + \xi_{t_m})^2 - \lambda\Lambda_{t_m} G(\dot{\varphi}_{t_m}^\theta) \right] / (N \times \text{batch_size})$;
16	Calculate the gradient of Loss with respect to θ ;
17	Back propagate updates for $\{\theta_m, m = 0, \dots, N\}$ via Adam (switch to SGD when fine tuning);
18	$epoch++$;
19	end
20	return: (local) optimizer $\theta^* = \{\theta_m^*, m = 0, \dots, N\}$.

In Algorithm 3, we use deep hedging algorithm to learn the optimal trading strategy starting at $T - \kappa\sqrt{\lambda}$ to maturity T , in order to have the scalability in both trading time horizon and dimension to work in cases where the trading time horizon is long and there are multiple stocks in the market. Based on the needs, other deep learning-based algorithms can also be applied starting $\kappa\sqrt{\lambda}$ before maturity T . Implementation details can be found here: <https://github.com/InnerPeas/ML-for-Transaction-Costs/blob/main/SingleAgent-Stage2/README.md>.

5 Conclusion and Looking-forward

This paper studies the optimal hedging problems in frictional markets with general convex transaction costs on the trading rates, and propose a simple pasting algorithm to fully utilize the leading-order asymptotic formula and the deep learning-based algorithms. Under the smallness assumption on the magnitude of the transaction costs, the leading order approximation of the optimal trading speed can be identified through the solution to a nonlinear SDE. Models with arbitrary state dynamics generally lead to a nonlinear FBSDE system, but we can still solve the optimization numerically through learning-based algorithms. We implement the FBSDE solver and the deep hedging algorithms and compare their performances with the leading order approximation. The leading-order approximation works well under long trading horizons, while it deviates from the ground truth by a significant amount only shortly before maturity. On the other hand, the FBSDE only performs well under short trading horizons, while it fails to work in long trading horizons. In contrast, the deep hedging algorithm has stable and reliable performance for short and moderately long trading horizons, while it starts to get unstable when the trading horizon is getting too large. In addition, the hyperparameter tuning of the deep hedging algorithm becomes inefficient when the model has more sophisticated dynamics. Therefore, we propose our algorithm when the time horizon is large to paste the leading-order asymptotic formula and learning-based algorithms together with time threshold $O(\sqrt{\lambda}/T)$. This work is also a preliminary documents for learning-based numerical solution to frictional equilibrium models.

References

- [1] V. V. Acharya and L. H. Pedersen. Asset pricing with liquidity risk. *J. Financ. Econ.*, 77(2):375–410, 2005.
- [2] L. Ahrens. On using shadow prices for the asymptotic analysis of portfolio optimization under proportional transaction costs. 2015.
- [3] R. F. Almgren. Optimal execution with nonlinear impact functions and trading-enhanced risk. *Appl. Math. Finance*, 10(1):1–18, 2003.
- [4] R. F. Almgren and N. Chriss. Optimal execution of portfolio transactions. *J. Risk*, 3:5–40, 2001.
- [5] R. F. Almgren and T. M. Li. Option hedging with smooth market impact. *Market Microstructure Liq.*, 2(1), 2016.
- [6] R. F. Almgren, C. Thum, E. Hauptmann, and H. Li. Direct estimation of equity market impact. *RISK*, July, 2005.
- [7] Y. Amihud, H. Mendelson, and L. H. Pedersen. Liquidity and asset prices. *Foundations and Trends in Finance*, 1(4):269–364, 2006.
- [8] S. Ankirchner and T. Kruse. Optimal position targeting with stochastic linear–quadratic costs. *Banach Center Publ.*, 104(1):9–24, 2015.
- [9] P. Bank, H. M. Soner, and M. Voß. Hedging with temporary price impact. *Math. Fin. Econ.*, 11(2):215–239, 2017.
- [10] E. Bayraktar, T. Cayé, and I. Ekren. Asymptotics for small nonlinear price impact: a PDE homogenization approach to the multidimensional case. *Math. Finance*, to appear, 2018.
- [11] C. Beck, M. Hutzenthaler, A. Jentzen, and B. Kuckuck. An overview on deep learning-based approximation methods for partial differential equations. *arXiv preprint arXiv:2012.12348*, 2020.
- [12] S. Becker, P. Cheridito, and A. Jentzen. Deep optimal stopping. *Journal of Machine Learning Research*, 20:74, 2019.
- [13] B. Bouchard, M. Fukasawa, M. Herdegen, and J. Muhle-Karbe. Equilibrium returns with transaction costs. *Finance Stoch.*, 22(3):569–601, 2018.
- [14] H. Buehler, L. Gonon, J. Teichmann, and B. Wood. Deep hedging. *Quantitative Finance*, 19(8):1271–1291, 2019.
- [15] H. Buehler, L. Gonon, J. Teichmann, B. Wood, B. Mohan, and J. Kochems. Deep hedging: hedging derivatives under generic market frictions using reinforcement learning. *Swiss Finance Institute Research Paper*, (19-80), 2019.
- [16] P. Casgrain, B. Ning, and S. Jaimungal. Deep q-learning for nash equilibria: Nash-dqn. *arXiv preprint arXiv:1904.10554*, 2019.

- [17] T. Cayé, M. Herdegen, and J. Muhle-Karbe. Trading with small nonlinear price impact. *Ann. Appl. Probab.*, to appear, 2018.
- [18] T. Cayé, M. Herdegen, and J. Muhle-Karbe. Trading with small nonlinear price impact. *Ann. Appl. Probab.*, to appear, 2019.
- [19] J. H. Choi and K. Larsen. Taylor approximation of incomplete Radner equilibrium models. *Finance Stoch.*, 19(3):653–679, 2015.
- [20] J. De Lataillade, C. Deremble, M. Potters, and J.-P. Bouchaud. Optimal trading with linear costs. *RISK*, 1(3):2047–1246, 2012.
- [21] F. Delarue. On the existence and uniqueness of solutions to fbsdes in a non-degenerate case. *Stochastic processes and their applications*, 99(2):209–286, 2002.
- [22] B. Dumas and E. Luciano. An exact solution to a dynamic portfolio choice problem under transactions costs. *J. Finance*, 46(2):577–595, 1991.
- [23] I. Ekeland and R. Temam. *Convex analysis and variational problems*. SIAM, Philadelphia, PA, 1999.
- [24] N. Garleanu and L. H. Pedersen. Dynamic trading with predictable returns and transaction costs. *J. Finance*, 68(6):2309–2340, 2013.
- [25] N. Garleanu and L. H. Pedersen. Dynamic portfolio choice with frictions. *J. Econ. Theory*, 165:487–516, 2016.
- [26] L. Gonon, J. Muhle-Karbe, and X. Shi. Asset pricing with general transaction costs: Theory and numerics. *Mathematical Finance*, 31(2):595–648, 2021.
- [27] I. Goodfellow, Y. Bengio, and A. Courville. *Deep Learning*. MIT Press, Cambridge, MA, 2016.
- [28] P. Grohs, F. Hornung, A. Jentzen, and P. von Wurstemberger. A proof that artificial neural networks overcome the curse of dimensionality in the numerical approximation of black-scholes partial differential equations. Preprint, 2018.
- [29] P. Guasoni, M. Rásonyi, et al. Hedging, arbitrage and optimality with superlinear frictions. *Ann. Appl. Probab.*, 25(4):2066–2095, 2015.
- [30] P. Guasoni and M. Weber. Dynamic trading volume. *Math. Finance*, 27(2):313–349, 2017.
- [31] P. Guasoni and M. H. Weber. Nonlinear price impact and portfolio choice. *Mathematical Finance*, 30(2):341–376, 2020.
- [32] J. Han, A. Jentzen, and W. E. Solving high-dimensional partial differential equations using deep learning. *Proc. Natl. Acad. Sci.*, 115(34):8505–8510, 2018.
- [33] J. Han and J. Long. Convergence of the deep bsde method for coupled fbsdes. *Probability, Uncertainty and Quantitative Risk*, 5(1):1–33, 2020.
- [34] J. Han and E. Weinan. Deep learning approximation for stochastic control problems. 2016.
- [35] M. Herdegen and J. Muhle-Karbe. Stability of radner equilibria with respect to small frictions. *Finance and Stochastics*, 22(2):443–502, 2018.
- [36] R. Hu. Deep fictitious play for stochastic differential games. *arXiv preprint arXiv:1903.09376*, 2019.
- [37] C. Huré, H. Pham, A. Bachouch, and N. Langrené. Deep neural networks algorithms for stochastic control problems on finite horizon, part i: convergence analysis. *arXiv preprint arXiv:1812.04300*, 2018.
- [38] K. Janeček and S. E. Shreve. Futures trading with transaction costs. *Illinois J. Math.*, 54(4):1239–1284, 2010.
- [39] J. Kallsen and S. Li. Portfolio optimization under small transaction costs: a convex duality approach. *arXiv preprint arXiv:1309.3479*, 2013.
- [40] J. Kallsen and J. Muhle-Karbe. The general structure of optimal investment and consumption with small transaction costs. *Math. Finance*, 27(3):659–703, 2017.
- [41] M. Kohlmann and S. Tang. Global adapted solution of one-dimensional backward stochastic Riccati equations, with application to the mean–variance hedging. *Stochastic Process. Appl.*, 97(2):255–288, 2002.
- [42] F. Lillo, J. D. Farmer, and R. N. Mantegna. Master curve for price-impact function. *Nature*, 421:129–130, 2003.
- [43] H. Liu. Optimal consumption and investment with transaction costs and multiple risky assets. *The Journal of Finance*, 59(1):289–338, 2004.
- [44] C. C. Moallemi and M. Wang. A reinforcement learning approach to optimal execution. 2021.
- [45] L. Moreau, J. Muhle-Karbe, and H. M. Soner. Trading with small price impact. *Math. Finance*, 27(2):350–400, 2017.
- [46] J. Muhle-Karbe, X. Shi, and C. Yang. An equilibrium model for the cross-section of liquidity premia. Preprint, November 2020.
- [47] J. M. Mulvey, Y. Sun, M. Wang, and J. Ye. Optimizing a portfolio of mean-reverting assets with transaction costs via a feedforward neural network. *Quantitative Finance*, 20(8):1239–1261, 2020.

- [48] Y. Nevmyvaka, Y. Feng, and M. Kearns. Reinforcement learning for optimized trade execution. In *Proceedings of the 23rd international conference on Machine learning*, pages 673–680, 2006.
- [49] A. M. Reppen and H. M. Soner. Bias-variance trade-off and overlearning in dynamic decision problems. *arXiv preprint arXiv:2011.09349*, 2020.
- [50] J. Ruf and W. Wang. Hedging with linear regressions and neural networks. *Journal of Business & Economic Statistics*, (just-accepted):1–33, 2021.
- [51] Y. Sannikov and A. Skrzypacz. Dynamic trading: price inertia and front-running. 2016. Preprint.
- [52] X. Shi. *Equilibrium asset pricing with transaction costs*. PhD thesis, Carnegie Mellon University, Pittsburgh, PA, USA, 2020.
- [53] S. E. Shreve and H. M. Soner. Optimal investment and consumption with transaction costs. *The Annals of Applied Probability*, pages 609–692, 1994.
- [54] H. M. Soner and N. Touzi. Homogenization and asymptotics for small transaction costs. *SIAM J. Control Optim.*, 51(4):2893–2921, 2013.
- [55] R. S. Sutton and A. G. Barto. *Reinforcement learning: An introduction*. MIT press, 2018.
- [56] H. Wang, T. Zariphopoulou, and X. Y. Zhou. Reinforcement learning in continuous time and space: A stochastic control approach. *J. Mach. Learn. Res.*, 21:198–1, 2020.
- [57] H. Wang and X. Y. Zhou. Continuous-time mean–variance portfolio selection: A reinforcement learning framework. *Mathematical Finance*, 30(4):1273–1308, 2020.

A Asymptotics Results

When the transaction costs is considered to be quadratic, i.e. $G(x) = x^2/2$, we are luck to have a linear function $(G')^{-1}(x) = x$. Hence the forward equation (2.13) becomes *linear* with respect to the backward component Y , and hence existence and uniqueness can be established as in [21, 41], provided the coefficients satisfies certain regularities. However, for general function G satisfying Assumption (2.1), the generator for the forward component is not globally Lipschitz hence no general theory is available for the FBSDE system (2.13) - (2.14).

A.1 A Concrete Example

As already emphasized above, a general existence proof for the FBSDE system (2.13) - (2.14) remains a challenging open problem. Let us just briefly sketch how the nonlinear FBSDE (2.13) - (2.14) reduces to a nonlinear PDE, with the following assumptions on the market:

- Assumption A.1.** (i) the frictionless strategy satisfies that $\bar{b}_t = 0$ and $\bar{a}_t = \bar{a}$;
- (ii) the volatility process of the stock price remain constant $\sigma > 0$ in the models with and without transaction costs;
- (iii) the cost parameter is constant ($\Lambda = 1$).

Under Assumption A.1, the forward-backward system (2.13) - (2.14) in turn becomes autonomous,

$$d\Delta\varphi_t = (G')^{-1}\left(\frac{Y_t}{\lambda}\right)dt - \bar{a}dW_t, \quad \Delta\varphi_0 = \varphi_{0-} + \frac{\xi_0}{\sigma} - \frac{\mu_0}{\gamma\sigma^2}, \quad (\text{A.1})$$

$$dY_t = \gamma\sigma^2\Delta\varphi_t dt + Z_t dW_t, \quad Y_T = 0. \quad (\text{A.2})$$

Now use the standard ansatz that the backward component Y_t should be a function $g(t, \Delta\varphi_t)$ of time and the forward component. Itô's formula and the dynamics of the forward component in turn yield:

$$dY_t = \left(\partial_t + (G')^{-1}\left(\frac{g}{\lambda}\right) \partial_x + \frac{\bar{a}^2}{2} \partial_{xx} \right) g(t, \Delta\varphi_t) dt - \bar{a} \partial_x g(t, \Delta\varphi_t) dW_t.$$

Comparing the drift rate to the BSDE (A.2), we therefore obtain the following semilinear PDE for the function $g(t, x)$:

$$\begin{cases} \partial_t g + (G')^{-1} \left(\frac{g}{\lambda} \right) \partial_x g + \frac{\bar{a}^2}{2} \partial_{xx} g = \gamma \sigma^2 x, & \text{in } x \in \mathbb{R}, t \in (0, T), \\ g(T, x) = 0, & \text{on } x \in \mathbb{R}. \end{cases} \quad (\text{A.3})$$

When $G(x) = x^2/2$, we know that g have the explicit form as:

$$g(t, x) = -\sqrt{\gamma \sigma^2 \lambda} x \tanh \left(\sqrt{\frac{\gamma \sigma^2}{\lambda}} (T - t) \right). \quad (\text{A.4})$$

In general, solving (A.3) is hard, letting alone having a solution explicitly. For the numerical solution of the PDE (A.3), however, it becomes incompatible with the zero terminal condition at maturity, which describes that trading slows down and eventually stops near the terminal time. For more general versions of the model, even the stationary boundary conditions in the space dimensions are not readily available and it is not clear how to paste them together with the terminal condition. Accordingly, it is not straightforward to solve the PDE (A.3) and its extensions using finite-difference schemes and the form of the PDE (A.3) can not fit in the deep-learning solver of [11].

A.2 Asymptotically Optimal Trading Strategies

In this section, we establish the asymptotic optimal strategy $\dot{\varphi} = (\dot{\varphi}_t)_{t \in [0, T]}$ for the frictional mean-variance preference (2.3). For better readability, we introduce the optimal strategy under Assumption A.1. The proof for the main approximation result is in Appendix B. We show that, under Assumption (A.1), the smallness assumption on the transaction costs level λ is a relative quantity with respect to the trading time horizon. We first introduce the following two ingredients for the asymptotic trading strategy.

A nonlinear ODE The first ingredient to cook up the strategy $\dot{\varphi}$ is the solution to a nonlinear ODE, which is also essential to the analysis of [26], Lemma 3.4 and the formal analysis of [52], Lemma 2.5.

Lemma A.2. *Suppose the instantaneous transaction cost G satisfies Assumption 2.1. Then the ordinary differential equation*

$$(G')^{-1} \left(\frac{g(x)}{\lambda} \right) g'(x) + \frac{\bar{a}^2}{2} g''(x) = \gamma \sigma^2 x. \quad (\text{3.5})$$

has a unique solution g on \mathbb{R} such that $xg(x) \leq 0$ for all $x \in \mathbb{R}$. Moreover, g is odd, non-increasing on \mathbb{R} and g satisfies the growth conditions

$$\lim_{x \rightarrow -\infty} \frac{g(x)}{\lambda(G^*)^{-1}(\frac{\gamma \sigma^2}{2\lambda} x^2)} = 1, \quad \lim_{x \rightarrow +\infty} \frac{g(x)}{\lambda(G^*)^{-1}(\frac{\gamma \sigma^2}{2\lambda} x^2)} = -1, \quad (\text{A.5})$$

where G^ is the Legendre transform of G .*

Remark A.3. For finite time horizons T , the PDE (A.3) cannot be reduced to an ODE. If the time horizon T is large, then the solution should become stationary ($\partial_t g(t, x) \approx 0$). Such a stationary

solution should in turn solve the following essential nonlinear ODE (3.5). Far from the terminal time T , it is natural to expect that the correct solution is still identified by the same growth condition in the space variable as (A.5).

For power functions $G(x) = |x|^q/q$, $q \in (1, 2]$, the Legendre transform is

$$G^*(x) = \sup_y \{xy - G(y)\} = x(G')^{-1}(x) - G((G')^{-1}(x)) = |x|^p/p,$$

where $p = q/(q - 1)$ is the conjugate of q . In this case, with proper inner and outer rescaling coefficients, (3.5) is exactly the *same* ODE which plays an important role in Lemma 19 and Lemma 21 in [31] and Lemma 3.1 in [18].

A fast mean-reverting SDE The second ingredient is the strong solution to a fast mean-reverting SDE.

Lemma A.4. *Let g be the solution of the ODE (3.5) from Lemma A.2. There exists a unique strong solution of the SDE*

$$d\Delta_t = (G')^{-1} \left(\frac{g(\Delta_t)}{\lambda} \right) dt - \bar{a}dW_t, \quad \Delta_0 = \varphi_{0-} + \frac{\xi_0}{\sigma} - \frac{\mu_0}{\gamma\sigma^2}. \quad (\text{A.6})$$

Moreover, this process is a recurrent diffusion.

Remark A.5. When $G(x) = x^2/2$, the solution to (3.5) is $g(x) = -\sqrt{\gamma\sigma^2\lambda}x$, and the dynamics (A.6) becomes

$$d\Delta_t = -\sqrt{\frac{\gamma\sigma^2}{\lambda}} \Delta_t dt - \bar{a}dW_t, \quad \Delta_0 = \varphi_{0-} + \frac{\xi_0}{\sigma} - \frac{\mu_0}{\gamma\sigma^2}, \quad (\text{A.7})$$

which follows Ornstein-Uhlenbeck process in this case. In general, the requirement of $xg(x) \leq 0$ ensures that the dynamic (A.6) is indeed mean-reverting and converges to an ergodic limit.

With these two ingredients on hand, we now present our first results in the following theorem:

Theorem A.6. *Let g be the solution to (3.5) and $(\Delta_t)_{t \geq 0}$ the solution to (A.6). Then under Assumption 2.1 and Assumption A.1, for all competing admissible strategies $\dot{\varphi}$, we have*

$$\sup_{\dot{\varphi}} J_T(\dot{\varphi}) = J_T \left((G')^{-1} \left(\frac{g(\Delta)}{\lambda} \right) \right) + O \left(\frac{\sqrt{\lambda}}{T} \right).$$

Theorem A.6 shows that, under Assumption A.1 the smallness is in fact on the quantity $\sqrt{\lambda}/T$, i.e. the smallness of λ is a relative quantity. When fluctuation in the transaction costs parameters or the frictionless strategy has a non-zero drift rate, the smallness is an absolute requirement on the liquidity level λ .

When the transaction costs is quadratic, i.e. $G(x) = x^2/2$, we can create the optimal strategy with the help of (A.4). Accordingly, the approximation can be made more precise, and we summarize the results as follows:

Corollary A.7. *For $G(x) = x^2/2$, define the optimal strategy*

$$\dot{\varphi}_t = -\sqrt{\frac{\gamma\sigma^2}{\lambda}} \tanh \left(\sqrt{\frac{\gamma\sigma^2}{\lambda}} (T - t) \right) \left(\varphi_{0-} + \frac{\xi_0}{\sigma} - \frac{\mu_0}{\gamma\sigma^2} - \int_0^t \frac{\bar{a} dW_u}{\cosh \sqrt{\frac{\gamma\sigma^2}{\lambda}} (T - u)} \right). \quad (\text{A.8})$$

Then under Assumption A.1, for all competing admissible strategies $\dot{\varphi}$, we have

$$\sup_{\dot{\varphi}} J_T(\dot{\varphi}) = J_T(\dot{\varphi}) = J_T \left(-\sqrt{\frac{\gamma\sigma^2}{\lambda}} \Delta \right) + O \left(\frac{\lambda}{T} \right),$$

where Δ is the solution to (A.7).

B Proof of Section A.2

The proof of Lemma A.2 follows the same procedure as the proof of Lemma 3.4 in [26], and Lemma A.4 follows the same procedure as the proof of Lemma 3.5 in [26].

Here we provide some auxiliary results on the function g from (3.5).

Corollary B.1. *Let g be the solution to (3.5) on \mathbb{R} with $xg(x) \leq 0$. Then the following holds:*

1. *There exists a constant $C_G > 0$ that only depends on G such that for all $x \in \mathbb{R}$,*

$$|g(x)| \leq C_G \sqrt{\lambda} \left(\sqrt{\lambda} + \sqrt{\gamma\sigma^2|x|} \right). \quad (\text{B.1})$$

2. *There exists a constant $K_G > 0$ that only depends on G such that for all $x \in \mathbb{R}$,*

$$|g'(x)| \leq \sqrt{\gamma\sigma^2\lambda} K_G. \quad (\text{B.2})$$

Proof of Theorem A.6. With the strategy, we write

$$\hat{\varphi}_t = \varphi_{0-} + \int_0^t (G')^{-1} \left(\frac{g(\Delta_u)}{\lambda} \right) du = \varphi_{0-} + \bar{\varphi}_t + \Delta_t - \left(\frac{\mu_0}{\gamma\sigma^2} - \frac{\xi_0}{\sigma} + \Delta_0 \right) = \bar{\varphi}_t + \Delta_t,$$

hence with (2.10), we have

$$\gamma\sigma^2\Delta_t = \gamma\sigma^2(\hat{\varphi}_t - \bar{\varphi}_t) = \gamma\sigma(\sigma\hat{\varphi}_t + \xi_t) - \mu_t. \quad (\text{B.3})$$

Consider a competing admissible strategy φ and, to ease notation, set

$$\dot{\theta}_t = \dot{\varphi}_t - (G')^{-1} \left(\frac{g(\Delta_t)}{\lambda} \right), \quad \text{so that} \quad \theta_t = \int_0^t \dot{\varphi}_u - (G')^{-1} \left(\frac{g(\Delta_u)}{\lambda} \right) du = \varphi_t - \hat{\varphi}_t.$$

Equation (B.3) and the convexity of G yield

$$\begin{aligned} & J_T(\dot{\varphi}) - J_T \left((G')^{-1} \left(\frac{g(\Delta)}{\lambda} \right) \right) \\ &= \frac{1}{T} \mathbb{E} \left[\int_0^T \theta_t \mu_t - \frac{\gamma}{2} \theta_t (\varphi_t \sigma + \hat{\varphi}_t \sigma + 2\xi_t) \sigma + \lambda \left(G \left((G')^{-1} \left(\frac{g(\Delta_t)}{\lambda} \right) \right) - G(\dot{\varphi}_t) \right) dt \right] \\ &\leq \frac{1}{T} \mathbb{E} \left[\int_0^T -\frac{1}{2} \gamma (\theta_t \sigma)^2 + \theta_t (\mu_t - \gamma(\hat{\varphi}_t \sigma + \xi_t) \sigma) + \lambda G' \left((G')^{-1} \left(\frac{g(\Delta_t)}{\lambda} \right) \right) \left((G')^{-1} \left(\frac{g(\Delta_t)}{\lambda} \right) - \dot{\varphi}_t \right) dt \right] \\ &= \frac{1}{T} \mathbb{E} \left[\int_0^T -\frac{1}{2} \gamma (\theta_t \sigma)^2 - \gamma \theta_t \sigma^2 \Delta_t - g(\Delta_t) \dot{\theta}_t dt \right]. \quad (\text{B.4}) \end{aligned}$$

We now analyze the terms on the right-hand side of (B.4). The dynamics (A.6) of Δ_t , Itô's formula, and the ODE (3.5) for g imply

$$dg(\Delta_t) = \left(g'(\Delta_t)(G')^{-1} \left(\frac{g(\Delta_t)}{\lambda} \right) + \frac{\bar{a}^2}{2} g''(\Delta_t) \right) dt - \bar{a}g'(\Delta_t)dW_t = \gamma\sigma^2\Delta_t dt - \bar{a}g'(\Delta_t)dW_t. \quad (\text{B.5})$$

Integration by parts and the dynamics (B.5) in turn yield

$$d[\theta_t g(\Delta_t)] = \left(\dot{\theta}_t g(\Delta_t) + \gamma\theta_t\sigma^2\Delta_t \right) dt - \bar{a}\theta_t g'(\Delta_t)dW_t. \quad (\text{B.6})$$

Here, the local martingale part is a true martingale. Indeed, by Hölder's inequality, the integrability condition $\varphi\sigma \in \mathbb{H}^2$ and the boundedness of g' established in Corollary B.1,

$$\mathbb{E} \left[\int_0^t |\theta_u g'(\Delta_u)|^2 du \right] \leq \gamma\sigma^2 \lambda K_G^2 \mathbb{E} \left[\int_0^t \theta_u^2 du \right] < \infty.$$

Also taking into account that

$$|g(\Delta_t)| \leq \sqrt{\gamma\sigma^2\lambda}C_G|\Delta_t| + \lambda C_G,$$

we can therefore use (B.6) to replace the second and the third terms on the right-hand side of (B.4), obtaining

$$J_T(\dot{\varphi}) - J_T(\dot{\varphi}) \leq -\frac{1}{T}\mathbb{E}[g(\Delta_T)\theta_T] - \mathbb{E} \left[\int_0^T \frac{\gamma}{2} (\theta_t\sigma)^2 dt \right].$$

The Cauchy-Schwartz inequality yields

$$\begin{aligned} |\mathbb{E}[g(\Delta_T)\theta_T]| &\leq (\mathbb{E}[g(\Delta_T)^2]\mathbb{E}[\theta_T^2])^{1/2} \\ &\leq (\mathbb{E}[2g(\Delta_T)^2](\mathbb{E}[(\varphi_T)^2] + \mathbb{E}[(\varphi_T)^2]))^{1/2} \\ &\leq 2C_G\sqrt{\lambda} (\mathbb{E}[(\varphi_T)^2] + \mathbb{E}[(\varphi_T)^2])^{1/2} (\gamma\sigma^2\mathbb{E}[|\Delta_t|^2] + \lambda)^{1/2}. \end{aligned}$$

Moreover, it follows that $\mathbb{E}[|\varphi_T|^2] = \mathbb{E}[|\Delta_T|^2] \leq \sup_{T \geq 0} \mathbb{E}[|\Delta_T|^2] < \infty$. Together with the transversality condition (2.5), it follows that

$$\frac{1}{T} |\mathbb{E}[g(\Delta\varphi_T^1)\theta_T]| \leq \frac{2C_G\sqrt{\lambda}}{T} (\mathbb{E}[(\varphi_T)^2] + \mathbb{E}[(\varphi_T)^2])^{1/2} (\gamma\sigma^2\mathbb{E}[|\Delta_t|^2] + \lambda) = O\left(\frac{\sqrt{\lambda}}{T}\right).$$

Therefore, the trading rate $\dot{\varphi}$ is indeed asymptotically optimal as:

$$\begin{aligned} \limsup_{\sqrt{\lambda}/T \rightarrow 0} J_T(\dot{\varphi}) - J_T(\dot{\varphi}) &\leq \limsup_{\sqrt{\lambda}/T \rightarrow 0} \frac{1}{T} \left[-\mathbb{E}[g(\Delta_T)\theta_T] - \mathbb{E} \left[\int_0^T \frac{\gamma}{2} (\theta_t\sigma)^2 dt \right] \right] \\ &= -\lim_{\sqrt{\lambda}/T \rightarrow 0} \frac{1}{T} \mathbb{E}[g(\Delta_T)\theta_T] + \limsup_{\sqrt{\lambda}/T \rightarrow 0} \frac{1}{T} \mathbb{E} \left[-\int_0^T \frac{\gamma}{2} (\theta_t\sigma)^2 dt \right] \leq 0. \end{aligned}$$

□